ELSEVIER

Ceramics International 31 (2005) 399–404

CERAMICS INTERNATIONAL

www.elsevier.com/locate/ceramint

# Investigation of electrical properties of tantalum doped $SnO_2$ varistor system

F.M. Filho[a], A.Z. Simões[a], A. Ries[a,*], E.C. Souza[a], L. Perazolli[a], M. Cilense[a], E. Longo[b], J.A. Varela[a]

[a]*Instituto de Química, UNESP, C.P. 355, 14800-900 Araraquara-SP, Brazil*
[b]*Laboratório Interdisciplinar de Eletroquímica e Cerâmica, Departamento de Química, UFSCar, C.P. 676,13565-905 São Carlos, SP, Brazil*

Received 26 January 2004; received in revised form 19 March 2004; accepted 2 June 2004
Available online 11 September 2004

**Abstract**

$Ta_2O_5$ doped $SnO_2$ varistor systems containing 0.5 mol% ZnO and 0.5 mol% CoO were prepared by mixed oxide method. Considering that ZnO and CoO oxides are densification additives only the $SnO_2$·ZnO·CoO ceramics cannot exhibit electrical nonlinearity. A small amount of $Ta_2O_5$ improves the nonlinear properties of the samples greatly. The height and width of the defect barriers were calculated. It was found that samples doped with 0.05 mol% $Ta_2O_5$ exhibit the highest density (98.5%), the lowest electric breakdown field ($E_b$ = 1100 V/cm) and the highest coefficient of nonlinearity ($\alpha$ = 11.5). The effect of $Ta_2O_5$ dopant could be explained by the substitution of $Ta^{5+}$ by $Sn^{4+}$. A grain-boundary defect barrier model for the $SnO_2$·ZnO·CoO·$Ta_2O_5$ varistor system was also introduced.


*Keywords:* E. Varistor; Tin dioxide; Tantalum oxide

## 1. Introduction

Varistors are ceramic semiconductor devices with highly nonlinear current–voltage characteristics similar to back-to-back Zener diodes but with much higher current and energy handling capabilities. Varistors based on ZnO have been most extensively studied [1–4]. At the same time, varistors based on other ceramic systems have also been under investigation, because of the need for better properties. One of these systems are the $SnO_2$-based varistors. Tin dioxide ($SnO_2$) is an n-type semiconductor with rutile type crystalline structure and has low densification rate due to its high surface tension as diffusion coefficient at low temperatures and high $SnO_2$ partial pressure at high temperatures [5]. Dense $SnO_2$-based ceramics can be achieved by introducing dopants or by hot isostatic pressure processing [6,7]. The addition of CoO creates oxygen vacancies and $Co'_{Sn}$ or $Co''_{Sn}$ which can segregate at the grain boundaries [8]. Both defects can help the formation of the Schottky barriers at grain boundaries. The function of ZnO is the creation of oxygen vacancies and $Zn''_{Sn}$ defects [9]. The latter are less segregated and contribute to the Schottky barrier formation. However, both additives lead to a highly resistive material. The addition of tantalum oxide creates $Ta_{Sn}^{\bullet}$ defect (donor) that increase the lattice conductivity of $SnO_2$ based ceramics [8]. Moreover, in small concentrations $Ta_2O_5$ does not segregate at the grain boundaries resulting in a high grain conductivity. Excess of $Ta_2O_5$ causes segregation of defects at grain boundaries which decrease both, bulk conductivity and grain size.

In our work, the $Ta_2O_5$ doped $SnO_2$ ceramics were prepared using ZnO and CoO as densification mediators. The effect of tantalum oxide on the physical and electrical properties of the $SnO_2$·ZnO·CoO varistors was

* Corresponding author.
*E-mail address:* ries750@yahoo.com.br (A. Ries).

0272-8842/$30.00 
doi:10.1016/j.ceramint.2004.06.004

investigated. As a result, an optimum composition was obtained.

## 2. Experimental procedure

The powder was prepared using the mixed oxide method in alcoholic medium. All the oxides used were analytical grade: $SnO_2$ (Cesbras-Fine), ZnO (Synth), CoO (Riedel), $Ta_2O_5$ (Aldrich). The molar composition of the investigated systems was $(99.00 - X)\%$ $SnO_2 + 0.50\%$ CoO + 0.50% ZnO + $X\%$ $Ta_2O_5$, with $X$ = 0.025, 0.050 and 0.075 mol%. The amounts of CoO and ZnO were always kept constant, because these additives promote densification during sintering. The dried powder was pressed into pellets by uniaxial pressing followed by isostatic pressing at 210 MPa. The pellets were sintered at 1400 °C for 2 h in oxygen atmosphere and slowly cooled to room temperature (5 °C/min). The tetragonal structure (rutile structure) of the $SnO_2$ starting material was confirmed by X-ray diffraction. All the X-ray data were collected with a Rigaku 2000 diffractometer under the following experimental conditions: copper anode, 50 kV, 150 mA, Cu Kα radiation monochromatized by a graphite crystal. Mean grain size was determined by analyzing the SEM micrographies (Topcom SM-300). To perform the electrical measurements, silver contacts were deposited on the sample surfaces. Current–tension measurements were taken using a High Voltage Measure Unit (KEITHLEY Model 237). The electric breakdown field ($E_b$) was obtained at a current density of 1 mA $cm^{-2}$. To investigate the properties of defect barriers, current density versus applied electrical field was recorded at different temperatures.

## 3. Results and discussion

### 3.1. General results

Fig. 1 shows the XRD analysis of a $SnO_2$ based varistor system with a molar concentration of 0.50% CoO + 0.50% ZnO and different amounts of $Ta_2O_5$. Besides the $SnO_2$ rutile phase, no secondary phase was observed. A sintering study combined with XRD results indicated that sintering at 1400 °C for 2 h are the optimal conditions to obtain crystalline, dense $Ta_2O_5$, CoO and ZnO doped $SnO_2$ varistors containing only the expected rutile phase. The amount of additives is too small for XRD detection because of the limit of the XRD equipment. All dopants introduced to the $SnO_2$ matrix probably lead to a stable solid solution according to Eqs. (1)–(3):

$$ZnO \xrightarrow{SnO_2} Zn''_{Sn} + V_O^{\bullet\bullet} + O_O^x \quad (1)$$

$$CoO \xrightarrow{SnO_2} Co''_{Sn} + V_O^{\bullet\bullet} + O_O^x \quad (2)$$

$$2\,Ta_2O_5 \xrightarrow{SnO_2} 4\,Ta_{Sn}^{\bullet} + V''''_{Sn} + 10\,O_O^x \quad (3)$$

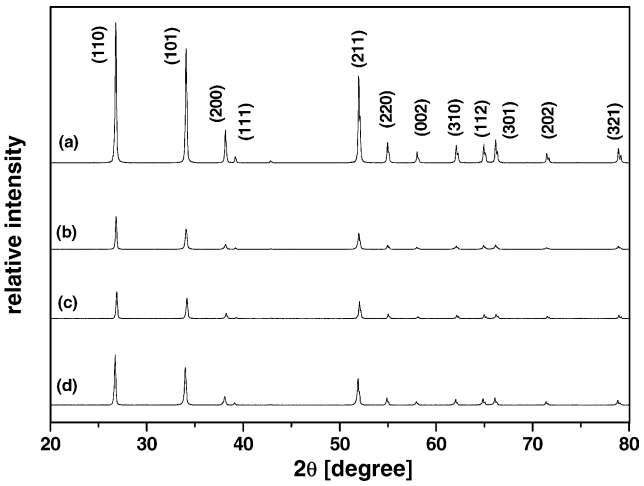


Fig. 1. X-ray diffraction data of the varistor system doped with different tantalum concentrations: (a) without Ta; (b) 0.025 mol%; (c) 0.050 mol%; and (d) 0.075 mol%.

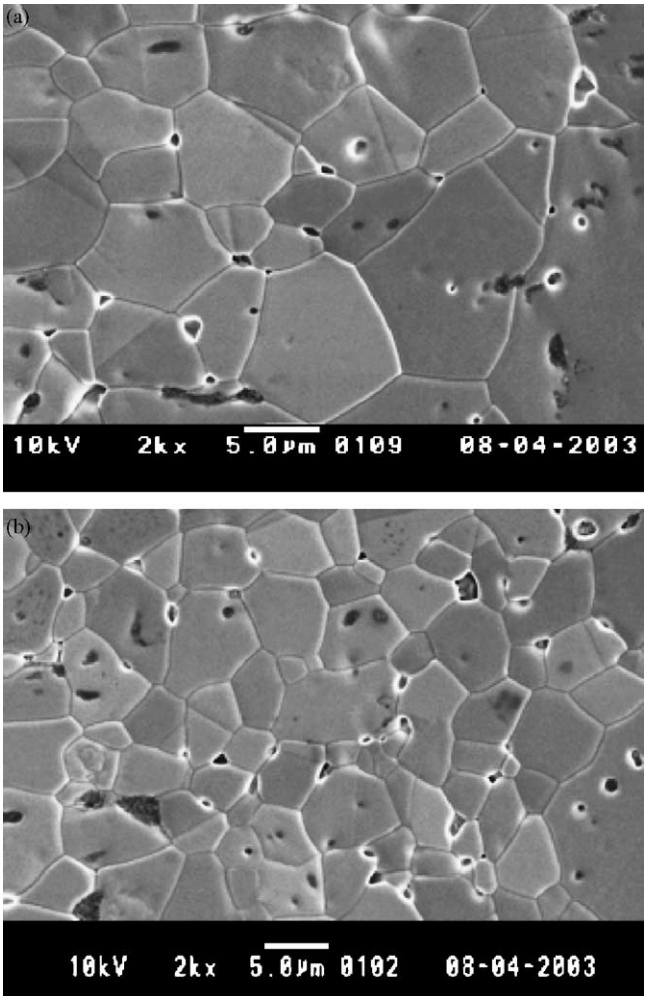


Fig. 2. SEM micrographs for SZC system doped with: (a) 0.05 mol% of $Ta_2O_5$ and (b) 0.075 mol% Ta.

The microstructure of the 0.05 and 0.075 mol% $Ta_2O_5$ doped $SnO_2$·ZnO·CoO ceramics are shown in Fig. 2. From the SEM micrographs it can be seen that no new apparent phase precipitation at the grain boundaries exist and the samples doped with 0.05 mol% $Ta_2O_5$ exhibit the highest grain size. Both samples present a uniform microstructure containing $SnO_2$ grains free of secondary phases. The relative densities of all samples exceeded 98% of the theoretical density.

The applied electric field as a function of current density for the different systems is given in Fig. 3. The nonlinear coefficient α was obtained by $\alpha = \log (I_2/I_1)/(V_2/V_1)$ where $V_1$ and $I_1$ as well as $V_2$ and $I_2$ are corresponding values of voltage and current for two points that can be chosen arbitrarily [10]. The $\alpha$ values were obtained from the curves $E$–$J$ for current densities chosen between 1 and 10 mA $cm^{-2}$. The highest nonlinear coefficient ($\alpha$ = 11.5) was obtained when molar concentrations of 0.05 mol% $Ta_2O_5$ were added to $SnO_2$, presenting an electric breakdown field of 1100 V/cm. For tantalum free samples no varistor behaviour was found, furthermore the material presented a low conductivity in agreement with low values of current density as shown in Fig. 3a.

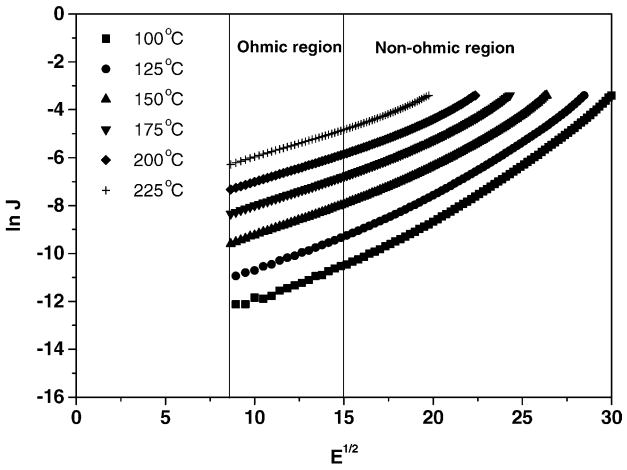


Fig. 4. Characteristic plot of ln $J$ vs. $E^{1/2}$ at different temperatures for the sample doped with 0.05 mol% $Ta_2O_5$.

Fig. 4 displays the characteristic of ln $J$ versus $E^{1/2}$ measured at different temperatures for the system containing 0.05 mol% of $Ta_2O_5$. As expected, the leakage current increases and the nonlinear coefficient $\alpha$ decreases with

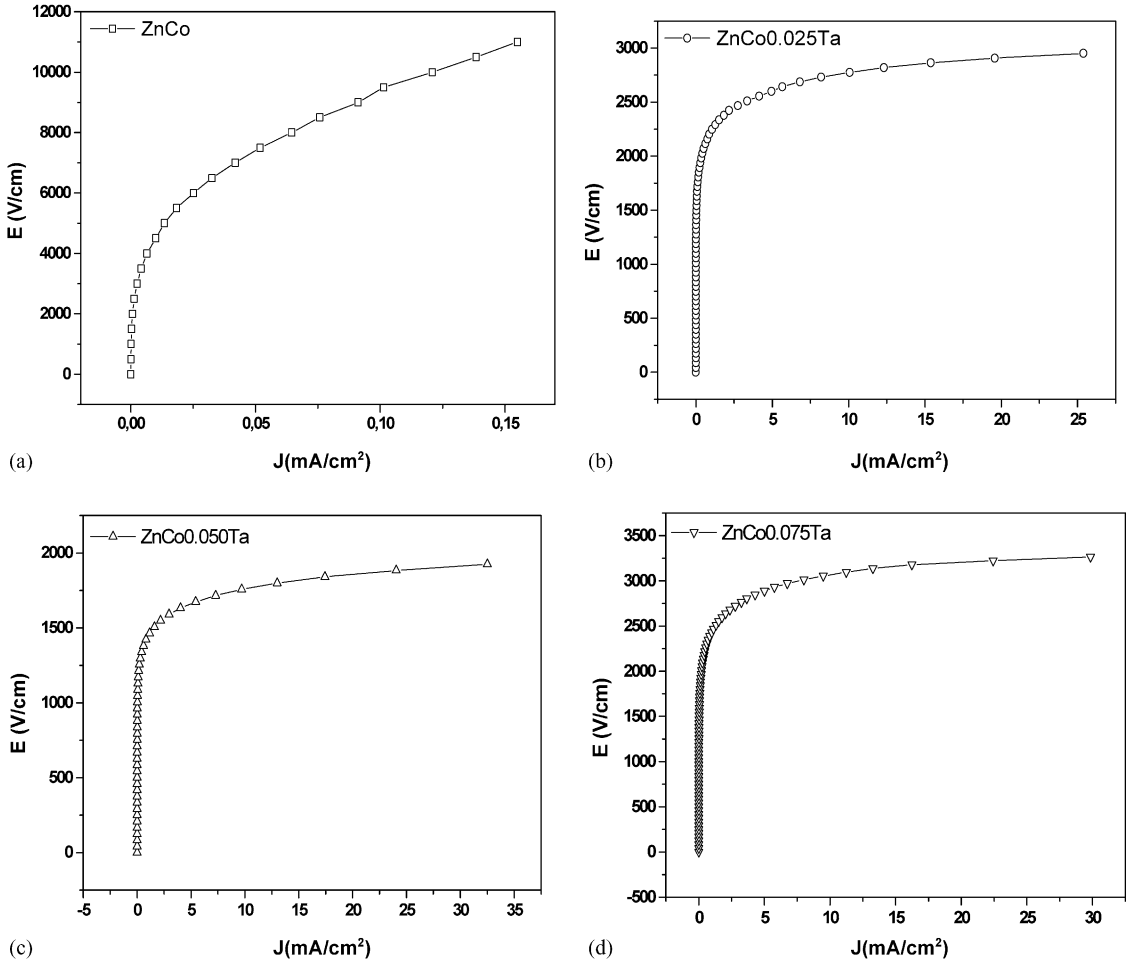


Fig. 3. Applied electric field as a function of current density for the SZC system doped with different tantalum concentrations: (a) without Ta; (b) 0.025 mol%; (c) 0.050 mol%; and (d) 0.075 mol%.

increasing temperature. For low values of $E$ these curves are straight lines and the extrapolation of these lines in the ohmic region to $E = 0$ gives the values of current density ($J_0$) for different temperatures (see Fig. 4). The electric varistor behavior is governed by the presence of electrical barriers at the grain boundaries of the ceramic material. The electric breakdown field $E_b$ depends on the average number of electrical barriers formed per unit length during sintering ($n$) and on the voltage barrier ($v_b$), which is for ZnO based varistors about 2 or 4 V/barrier [11,12]. Thus, the following equation relates $v_b$ and $E_b$:

$$E_b = nv_b \tag{4}$$

Considering that $L$ is the thickness of a cylindrical sample and $G$ is the mean grain size, the effective barrier voltage ($v_b$) is given by:

$$v_b = \frac{E_b G}{L} \tag{5}$$

Therefore, an increase in $E_b$ with a decrease in $G$ would be expected, keeping $v_b$ constant. However, the electric breakdown field is reduced from 1100 to 37 V/cm when the temperature is increased from 25 to 250 °C, as observed in Table 1. These results can be explained by an increase in the conductivity of the varistor system with the increase of temperature resulting in low values of the nonlinear coefficient ($\alpha$). For $Ta_2O_5$ concentration higher than 0.05 mol% an increase in $E_b$ was observed due to a possible tantalum segregation in the grain boundary which leads to a decrease in the grain size. These results clearly indicate a strong dependence of the electric breakdown field with the grain size. The addition of $Ta_2O_5$ to $SnO_2$ could produce a similar effect than $Nb_2O_5$ in the $SnO_2{\cdot}ZnO{\cdot}Nb_2O_5$ system studied by Pianaro et al. [13]. If so, these effects can be explained considering the following defect formation reactions:

$$V_{Sn}'''' + 2\,V_O \rightarrow V_{Sn}^{x} + 2\,V_O^{x} \tag{6}$$

$$2\,O_O^{x} + V_{Sn}^{x} \rightarrow O_2 + 2\,V_O + V_{Sn}'''' \tag{7}$$

As observed in Eq. (3), $Ta^{5+}$can replace $Sn^{4+}$ ions producing tin vacancies. These vacancies could react with intrinsic $SnO_2$ oxygen vacancy defects as represented by Eq. (6). Otherwise, $SnO_2$ lattice oxygen can react according to Eq. (7), restoring the oxygen vacancies and producing tin vacancies [14].

The electrical behavior of all samples at low electric field strengths is similar (Fig. 4) and the electric conduction is of the thermionic type. In this kind of emission the current density has an exponential dependence with temperature, according to the following equation [15]:

$$J = J_0 \exp\left(-\frac{E_a}{KT}\right) \tag{8}$$

where $J_0$ is a constant, $E_a$ the activation energy for the electron jump, $K$ the Boltzman constant and $T$ is the absolute temperature. Considering that the potential barriers are Schottky type separated by thin film and that the conduction mechanism is thermionic emission, the current density is related to the electric field $E$, by the following equation [16]:

$$J_s = A^* T^2 \exp\left[\frac{-(\phi_b - \beta E^{1/2})}{KT}\right] \tag{9}$$

where $A^*$ is the Richardson constant, $\phi_b$ the electric potential barrier height formed at the interface region, $E$ the electric field and $\beta$ is a constant related to the potential barrier width, $w$. The constant $\beta$ is given by:

$$\beta = \left[\left(\frac{1}{n_s \omega}\right)\left(\frac{2e^3}{4\pi\varepsilon_o\varepsilon_r}\right)\right]^{1/2} \tag{10}$$

where $n$ is the number of grains per unit length, $e$ the electron charge, and the product $\varepsilon_o\varepsilon_r$ is the material dielectric permittivity, respectively. The variable $n_s$ can be calculated by:

$$n_s = \frac{L}{d} \tag{11}$$

where $L$ is the sample thickness and $d$ is the mean grain size of $SnO_2$ varistor determined from the SEM micrograph.

The plot of ln $J$ as function of $1/T$ is a straight line as presented in Fig. 5 and the slope of this curve gives the activation energy for electronic transport. The potential barrier height ($\phi_b$) measured was 0.95 eV while the constant $\beta$ was found to be $4.37 \times 10^{-3}$ V$^{1/2}$ cm$^{1/2}$.

Table 1 shows that the samples doped with 0.05 mol% $Ta_2O_5$ exhibit the best nonlinear electrical properties due to the highest grain size, which decreases the electric breakdown field. Moreover, the samples doped with 0.05 mol% Ta also exhibit the highest density.

Table 1
Influence of temperature on the electrical properties of the $SnO_2{\cdot}ZnO{\cdot}CoO$ varistors doped with 0.05 mol% $Ta_2O_5$

| $Ta_2O_5$ concentration | $T$ (°C) | $\rho_r$ (%) | $E_b$ (V/cm) at 1 mA/cm$^2$ | $I_l$ (A) | $\alpha$ | Grain size (μm) ± 1% | $v_b$ (V/barrier) |
|---|---|---|---|---|---|---|---|
| 0.025 | 25 | 96.1 | 2440 | $2.1 \times 10^{-5}$ | 10.9 | 7.0 | 1.70 |
| 0.05 | 25 | 98.5 | 1100 | $2.8 \times 10^{-5}$ | 11.5 | 13.5 | 1.49 |
| 0.05 | 100 | – | 603 | $1.6 \times 10^{-4}$ | 7.2 | – | 0.81 |
| 0.05 | 150 | – | 376 | $3.8 \times 10^{-4}$ | 4.5 | – | 0.51 |
| 0.05 | 200 | – | 248 | $6.5 \times 10^{-4}$ | 2.1 | – | 0.33 |
| 0.05 | 250 | – | 37 | $7.3 \times 10^{-4}$ | 1.2 | – | 0.05 |
| 0.075 | 25 | 97.4 | 1900 | $4.4 \times 10^{-5}$ | 9.9 | 9.8 | 1.86 |

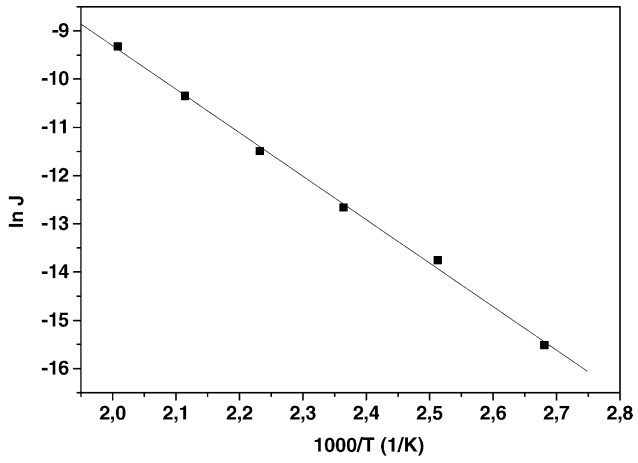


Fig. 5. Characteristic plot of ln $J$ against $1/T$ for $E = 0$ for the sample doped with 0.05 mol% $Ta_2O_5$.

### 3.2. Effect of dopants

Because there are no apparent secondary phases precipitated at the grain boundaries, defect formation by CoO and $Ta_2O_5$ in the $SnO_2$ matrix should be responsible for the origin of the potential barriers at grain boundaries. Thus, similar to the $SnO_2{\cdot}CoO{\cdot}Nb_2O_5$ based varistors the following equilibrium reaction may be suggested [15,16]:

$$CoO \xrightarrow{SnO_2} Sn''_{Sn} + V_O^{\bullet\bullet} + O_O^x \quad (12)$$

Considering that $SnO_2$ crystallizes in a tetragonal structure similar to rutile and that the ionic radius of $Co^{2+}$ ($r = 0.072$ μm) is similar to the ionic radius of $Sn^{4+}$ ($r = 0.071$ μm) there are interstitial sites that could accommodate foreign ions. These facts would facilitate the formation of oxygen vacancies, which determines the sintering kinetics, and the formation of solid solution by substituents or by interstitials, leading to the high shrinkage rate and densification of the $SnO_2{\cdot}ZnO{\cdot}CoO{\cdot}Ta_2O_5$ system:

$$CoO \xrightarrow{SnO_2} Co''_{Sn} + V_O^{\bullet\bullet} + O_O^x \quad (13)$$

The oxygen vacancies can combine with tin vacancies according to the reaction:

$$Vo''_{Sn} + V'''\prime_{Sn} \xrightarrow{SnO_2} Vo_{Sn}{}^{\bullet\bullet} + V''_{Sn} \quad (14)$$

Without the addition of tantalum oxide, the sample shows insulator behaviour, because of the high grain resistivity. The introduction of $Ta^{5+}$ in small amounts to the $SnO_2$ ceramics leads to the concentration of electrons and $V'''\prime_{Sn}$, which increases the electric conductivity in the $SnO_2$ lattice and leads to semiconductivity of the grains (see Eq. (3)). Moreover, the increase in the concentration of oxygen vacancies induced by the substitution of $Sn^{4+}$ by $Co^{2+}$ and $Ta^{5+}$ will also have an important effect on the decrease in grain resistivity because of the higher probability of electron hoping. A reduced grain resistivity facilitates the transport of electrons and other defect ions, which promote the densification of the samples. According to [17] with the substitution of $Sn^{4+}$ by $Ta^{5+}$ and $Co^{2+}$, together with the diffusion of oxygen vacancies the acceptor ions also tend to segregate in grain-boundary areas, especially during cooling. This increases the acceptor concentration (density of surface states, $N_s$) and results in high values of $\phi_B$ and $\omega$:

$$N_s = 2\omega N_d \quad (15)$$

$$\phi_B = q^2 N_s = 2\varepsilon_s N_d \quad (16)$$

$$\omega = \left(\frac{2\varepsilon_s \phi_B}{q^2 N_d}\right)^{1/2} \quad (17)$$

where $N_d$ is the donor density, $q$ the electric charge and $\varepsilon_s$ is the dielectric constant of the material. It is well known that the excess of oxygen produced during the sintering process provides the oxygen air for the sintering process. The oxygen could also be responsible for the Schottky barrier formation if it is considered that oxygen can be adsorbed at the interfaces and react with negative defects according to the following equations [18]:

$$\frac{1}{2}O_2 \rightarrow O_{ad}^x \quad (18)$$

$$2\,O_{ad}^x + V_{Sn}^{4-} \rightarrow 2\,O^- + V_{Sn}^{2-} \quad (19)$$

$$2\,O_{ad}^x + Sn_{Sn}^{2-} \rightarrow 2\,O^- + Sn_{Sn}^x \quad (20)$$

$$V_{Sn}^{4-} + 4\,O^- \rightarrow 4\,O^{2-} + V_{Sn}^x \quad (21)$$

$$2\,O^- + Sn_{Sn}^{2-} \rightarrow 2\,O^{2-} + Sn_{Sn}^x \quad (22)$$

It is well known from the literature that the adsorbed oxygen captures electrons from negatively charged acceptor defects at the grain boundaries and stays at this interface promoting the formation of Schottky barriers. Besides the function in the formation of boundary barriers, the dopants $Ta^{5+}$ and $Co^{2+}$ also create the sites to promote the adsorption of non-electrophilic species, $O^-$ and $O^{2-}$, which further promote the nonlinearity of $SnO_2$ varistors. Because of the possible segregation of $Ta^{5+}$ at the grain boundaries and the formation of grain-boundary barriers, the grain growth will be hindered to some extent. Thus, the grain size decreases with increase in $Ta_2O_5$ addition, which was verified by SEM. However, there is maximum solubility of the dopant in the system. When the tantalum oxide exceed this limit (0.05 mol%), the extra $Ta^{5+}$ will concentrate in the exterior of the grains, which will block the formation and transportation of electrons and other defects. Thus, it hinders the substitution and segregation of dopants, which inhibits the densification and the formation of the grain-boundary barriers.

### 3.3. Barriers model

Considering the microstructure of the $SnO_2$ varistor, an electric barrier of the Schottky type can be attributed to the

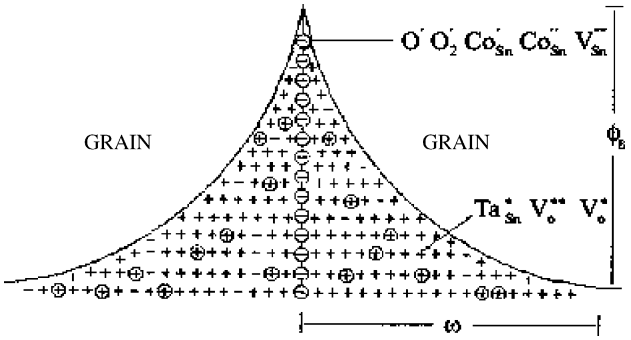


Fig. 6. The grain-boundary defect barrier model for $SnO_2$·ZnO·CoO·$Ta_2O_5$ varistors.

$SnO_2$ grain boundaries. The model presented in Fig. 6 proposes that the donors (positive charges) are distributed on both sides of the grain boundary and are compensated by acceptors (negative charges) at the interface of the grain boundary. Oxygen can be responsible for the formation of a Schottky barrier, provided that it can be adsorbed at the interface and react with the negative defects, according to the reactions below:

$$Co'_{Sn} + O_{2(ads)} \rightarrow O'_{2(ads)} + Co^{x}_{Sn} \quad (23)$$

$$Co''_{Sn} + O_{2(ads)} \rightarrow 2O'_{2(ads)} + Co^{x}_{Sn} \quad (24)$$

$$Co'_{Sn} + O_{2(ads)} \rightarrow 2O'_{2(ads)} + Co^{x}_{Sn} \quad (25)$$

$$Co''_{Sn} + 2O'_{2(ads)} \rightarrow 4O'_{2(ads)} + Co^{x}_{Sn} \quad (26)$$

These reactions are important to explain the voltage barrier formation at the grain boundaries, for a better understanding of the varistor behavior and the mechanisms that lead to this behavior. It can be proposed that the potential barrier is formed by the presence of trap states which are related to oxygen species ($O'_2$ and $O'$) at the grain boundary interfaces due to defects such as $Co'_{Sn}$ that transfer electrons to oxide ions.

## 4. Conclusions

$Ta_2O_5$ doped $SnO_2$ varistors were prepared by the mixed oxide method. The physical characterization showed that all the systems are well-densified ceramics. The experimental results indicated that $\alpha$ and $E_b$ of the SZC varistor system depend on the $Ta_2O_5$ concentration. The addition of $Ta_2O_5$ until 0.05 mol% increases the electric conductivity due to $V'''_{Sn}$ formation. Higher concentrations, however, decrease these properties reducing the number of trap states at the grain boundaries, possibly due to segregation of $Ta^{5+}$ at grain boundaries. The measured potential barrier height was 0.95 eV for the sample doped with 0.05 mol% in Ta. A double barrier model with no thin film between the grains is proposed to explain the nonohmic behavior of the $SnO_2$·ZnO·CoO·$Ta_2O_5$ based $SnO_2$ varistors.

## Acknowledgment

Financial support from the Brazilian agencies FAPESP, CNPq, and CAPES and the German Academic Exchange Service (DAAD) is gratefully acknowledged.

## References

[1] L.M. Levinson, H.R. Philipp, The physics of metal oxide varistors, J. Appl. Phys. 46 (1975) 1332–1334.
[2] P.R. Emtage, The physics of zinc oxide varistors, J. Appl. Phys. 48 (1977) 4372–4384.
[3] G.D. Mahan, L.M. Levinson, H.R. Philipp, Theory of conduction in ZnO varistors, J. Appl. Phys. 50 (1979) 2799–2812.
[4] D.R. Clarke, Varistor ceramics, J. Am. Ceram. Soc. 82 (1999) 485–502.
[5] Z.M. Jarzebski, J.P. Marton, Physical properties of $SnO_2$ materials, J. Electrochem. Soc. 123 (1976) C100–C205.
[6] J.A. Varela, O.J. Whittemore, E. Longo, Pore size evolution during sintering of ceramic oxides, Ceram. Int. 16 (1990) 177–189.
[7] T. Kimura, S. Inada, T. Yamaguchi, Microstructure development in $SnO_2$ with and without additives, J. Mater. Sci. 24 (1989) 220–226.
[8] J.A. Cerri, E.R. Leite, D. Gouvea, E. Longo, Effect of cobalt (II) oxides and manganese (IV) oxides on sintering of tin (IV) oxide, J. Am. Ceram. Soc. 79 (1996) 799–804.
[9] A.C. Antunes, S.R.M. Antunes, S.A. Pianaro, M.R. Rocha, E. Longo, J.A. Varela, Nonlinear electrical behavior of the $SnO_2$·CoO·$Ta_2O_5$ system, Mater. Sci. Lett. 17 (1988) 577–579.
[10] T.K. Gupta, Application of zinc oxide varistors, J. Am. Ceram. Soc. 73 (1990) 1817–1840.
[11] L.F. Lou, Current–voltage characteristics of ZnO–$Bi_2O_3$ heterojunction, J. Am. Ceram. Soc. 50 (1979) 555–558.
[12] G.D. Mahan, L.M. Levisnson, H.R. Philipp, Single grain junction studies of ZnO varistors—theory and experiment, Appl. Phys. Lett. 33 (1978) 830–832.
[13] S.A. Pianaro, P.R. Bueno, E. Longo, J.A. Varela, A new $SnO_2$ based varistor system, Mater. Sci. Lett. 14 (1995) 692–694.
[14] C.N. Turton, T.I. Turton, The Oxide Handbook, IFI/Plenum, New York, 1973, pp. 378–379.
[15] S.A. Pianaro, P.R. Bueno, E. Longo, J.A. Varela, Electrical properties of the $SnO_2$ based varistor, J. Mater. Sci.: Mater. Electron. 9 (1998) 159–165.
[16] Y.J. Wang, J.F. Wang, C.P. Li, Improved varistor nonlinearity via sintering and acceptor impurity doping, Eur. Phys. J. Appl. Phys. 11 (2000) 155–158.
[17] S.A. Pianaro, P.R. Bueno, E. Longo, J.A. Varela, Effect of $Bi_2O_3$ addition on the microstructure and electrical properties of the $SnO_2$·$Nb_2O_5$ varistor system, J. Mater. Sci. Lett. 16 (1997) 634–638.
[18] Y. Wang, Z. Aburas, K.L. Yao, Z.L. Liu, Effects of doping and temperature on nonlinearity of $WO_3$ varistor, Mater. Chem. Phys. 58 (1999) 51–54.